Wheel Control Based on Body Configuration for Step-Climbing Vehicle

Daisuke Chugo[1] , Kuniaki Kawabata[2] , Hayato Kaetsu[3] , Hajime Asama[4] and Taketoshi Mishima[5]

[1] The University of Tokyo, 2-11-16, Yayoi, Bunkyo-ku, Tokyo, Japan
chugo@iml.u-tokyo.ac.jp
[2] RIKEN (The Institute of Physical and Chemical Research), 2-1, Hirosawa, Wako-shi, Saitama,Japan kuniakik@riken.jp
[3] RIKEN (The Institute of Physical and Chemical Research), 2-1, Hirosawa, Wako-shi, Saitama,Japan kaetsu@riken.jp
[4] The University of Tokyo, 5-1-5, Kashiwanoha, Kashiwa-shi, Chiba, Japan
asama@race.u-tokyo.ac.jp
[5] Saitama University, 255, Shimo-Ookubo, Saimata-shi, Saitama, Japan
mishima@me.ics.saitama-u.ac.jp

Summary. In our current research, we are developing a holonomic mobile vehicle which is capable of running over the step. This system realizes omni-directional motion on flat floor using special wheels and passes over the step in forward or backward direction using the passive suspension mechanism. This paper proposes a new wheel control method of the vehicle according to its body configuration for passing over the step. The developed vehicle utilizes the passive suspension mechanism connected by two free joints that provide to change the body configuration on the terrain condition. Therefore, it is required to coordinate the suitable rotation velocity of each wheel according to its body configuration. In our previous work, the vehicle motion during step-climbing was discussed and moving velocity of each wheel was derived. In this paper, we adapt these results to wheel control and derived rotation velocity reference of each wheel. The performance of our proposed method is verified by the computer simulations and experiments using our prototype vehicle.

Keywords: Omni-Directional Mobile System, Passive Linkage Mechanism, Step-Climbing, Wheel Control

1 Introduction

In recent years, mobile robot technologies are expected to perform various tasks in general environment such as nuclear power plants, large factories, welfare care facilities and hospitals. However, there are narrow spaces with small barriers such as steps and the vehicle is required to have quick mobility

P. Corke and S. Sukkarieh (Eds.): Field and Service Robotics, STAR 25, pp. 331–342, 2006.

for effective task execution in such environments. The omni-directional mobility is useful for moving in narrow spaces, because there is no holonomic constraint on its motion. [1] [2] Furthermore, the step-overcoming function is necessary when the vehicle runs in the environment with barriers. In related works, various types of omni-directional mobile systems are proposed (legged robots, ball-shaped wheel robots, crawler robots, and so on). The legged robot [3] [4] can move in all directions and passes over rough terrain. However, its energy efficiency is not so good because the mechanisms tends to be complicated and the robot need to use its actuators in order to only maintain its posture. The robot with ball-shaped wheels can run in all directions [5], however, it cannot run on the rough grounds. The special crawler mechanism [6] is also proposed for the omni-directional mobile robot, but which can climb over only small steps. Therefore, there is still a lack of well-adapted mobile system for both narrow spaces and irregular terrain operation and we are developing a holonomic omni-directional vehicle with step-climbing ability. [7]

Our prototype mechanism consists of seven special wheels with free rollers (Figure 1) and a passive suspension mechanism. The special wheel equips twelve cylindrical free rollers [8] and applies the traction force only in advance direction. All special wheels are actuated and generate the omni-directional motion with suitable wheel arrangement and wheel control.

Furthermore, our mechanism utilizes new passive suspension system, which is more suitable for the step than general rocker-bogie suspensions. [9] [10] The free joint point 1 is in the same height as the axle and this system helps that the vehicle can pass over the step smoothly when the wheel contacts it in forward or backword direction. [7] No sensors and no additional actuators are equipped to pass over the barriers on the floor.

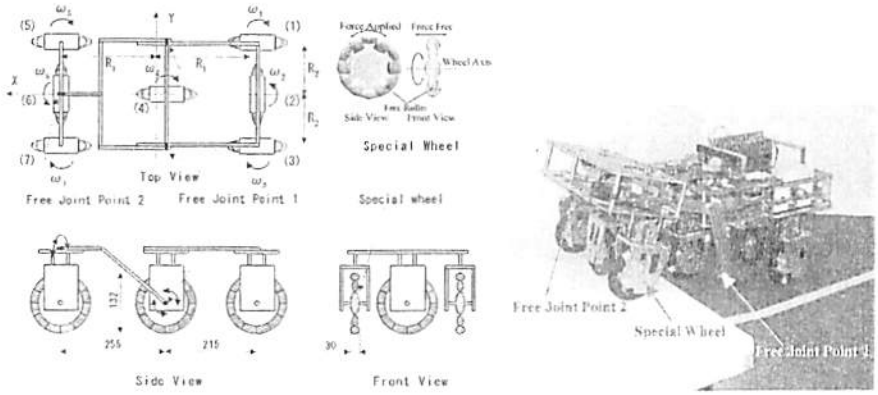

(a) Overview of the mechanism (b) Prototype vehicle

Fig. 1. Our prototype mechanism

Our prototype has redundant actuations, therefore the vehicle controller calculates the control reference of each wheel based on the kinematic model [11] and controls each actuator to take the coordination among the wheels using PID-based control.[12] When the vehicle with passive linkages overcomes the step, the moving velocity of each wheel is different because of the change of the body configuration and its kinematic model. Therefore, it is required to modify the wheel control reference referring to the change of its body configuration. However, in many cases, fixed control reference which is derived without the consideration of body configuration is adapted and it causes the wheel slippage or rotation error. [13]

In our previous work, we developed PID based control scheme with coordination among the wheel [12] and derived its control reference referring to its body shape. [14] However, wheel control reference tends to become too extraordinary, especially during step-climbing, because it is derived from only vehicle's body configuration without consideration of the balance among wheel velocities. Too extraordinary control reference causes wheel slippage and rotation error. Wheel slippage disturbs the vehicle mobile performance and it is important to reduce it for maximizing traction force. [15] Therefore, it is required to derive the suitable wheel control reference not only referring the body configuration but also maintaining the balance among the wheel rotation velocities. In this paper, we developed the adjusting method of wheel control reference referring to the modification of the body shape for reducing wheel slippage and rotation error, and increasing the mobile performance.

2 Control System

2.1 Kinematics

Our vehicle has the passive suspension mechanism in its body and the body configuration changes according to the terrain condition when the vehicle passes over the non-flat ground. Therefore, it is required to modify the wheel control referring to its configuration.

In this section, we consider the relationship of rotation velocity vector of each wheel and the change of the body configuration on general passive linkage vehicle model. We assume that the vehicle has n passive linkages and all wheels have grounded and actuated. When the vehicle passes over the barrier as shown in Figure 2 (a), the velocity vector of wheel $i+1$ is calculated by the velocity vector of wheel i and the rotation vector of wheel $i+1$ in equation (1). These vectors are expressed by three dimensions in their local coordination system.

$$\mathbf{v}_{i+1} = {}^{i}\mathbf{v}_{i} + {}^{i}\sigma_{i} \times {}^{i}\mathbf{P}^{i}_{i+1} \tag{1}$$

where i is the number of wheel ($i = 1 \cdots n$), ${}^{i}\mathrm{v}_i$ and ${}^{i}\sigma_i$ are the velocity vector and the rotation vector of wheel i on the coordinate system i, respectively. ${}^{i}\mathrm{P}^{i}_{i+1}$ is the position vector from the wheel i to wheel $i+1$ on coordination i.

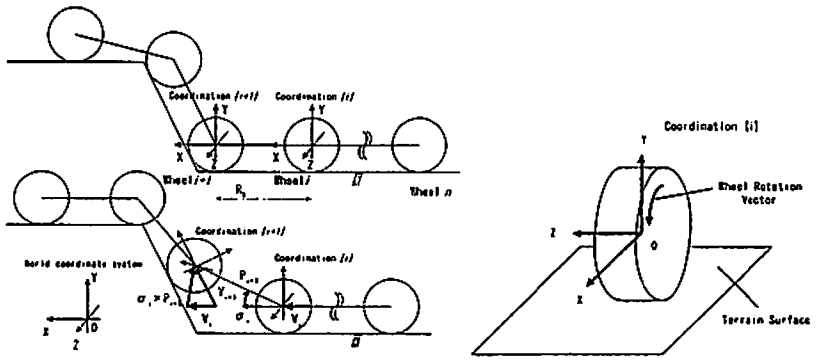

(a) Body configuration (b) Wheel model

Fig. 2. Relationship between the velocity vector and the vehicle body

The coordinate system of each wheel is defined as shown in Figure 2(b).
- The x-axis is defined in the drive direction of the wheel.
- The y-axis is defined in the perpendicular direction to the ground.

Thus, the x-direction ingredient of the velocity vector in the coordination {i} is derived as the control reference value. The control reference of the wheel $i+1$ (ω_{i+1}) is derived from equation (2) and (3).

$$\omega_{i+1} = \frac{\left\| {}^{i+1}\mathrm{v}_{i+1} \right\|_x}{r} + \left\| {}^{i}\sigma_i \right\|_z \tag{2}$$

$${}^{i+1}\mathrm{v}_{i+1} = {}^{i+1}_{i}\mathrm{R} \cdot {}^{i}\mathrm{v}_{i+1} \tag{3}$$

$\left\| {}^{i+1}\mathrm{v}_{i+1} \right\|_x$ is x ingredient of the wheel $i+1$ velocity vector, r is the radius of the wheel and ${}^{i+1}_{i}\mathrm{R}$ is the conversion matrix from the coordination $\{i\}$ to $\{i+1\}$. Thus, when the velocity vector and rotation vector of wheel i are defined as ${}^{i}\mathrm{v}_i$ and ${}^{i}\sigma_i$, the control reference of wheel $i+1$ is expressed as equation (4).

$$\omega_{i+1} = \frac{\left\| {}^{i+1}_{i}\mathrm{R} \cdot \left({}^{i}\mathrm{v}_i + {}^{i}\sigma_i \times {}^{i}\mathrm{P}^{i}_{i+1} \right) \right\|_x}{r} + \left\| {}^{i}\sigma_i \right\|_z \tag{4}$$

All wheels have grounded, therefore we can assume that each wheel grounds the plane as shown in Figure 2(b). When the angle between the x-axis of coordination {i} and the one of coordination {i+1} is α, the conversion matrix is derived as equation (5). α fulfills the equation (6).

$$ {}^{i+1}_{i}\mathrm{R} = \begin{bmatrix} \cos\alpha & -\sin\alpha & 0 \\ \sin\alpha & \cos\alpha & 0 \\ 0 & 0 & 1 \end{bmatrix} \tag{5} $$

$$ \left\| {}^{i+1}\mathrm{v}_{i+1} \right\|_{y} = 0 \tag{6} $$

2.2 Adaptation to Our Prototype

In previous section, we discuss the general vehicle kinematics referring to the body configuration. In this section, we adapt it to our prototype vehicle and derive the velocity vector of each wheel. Our vehicle measures the change of body configuration using its attitude sensors and generates the wheel control reference with this information.

Our vehicle has two potentiometers on each passive joint and tilt sensors which are attached on the rear part of the vehicle body as shown in Figure 3(a). We can measure the following angles using these sensors.

- The roll angle θ_1 and pitch angle γ_1 from potentiometers.
- The roll angle θ_2 and pitch angle γ_2 from tilt sensors.

Our developing vehicle has 7 wheels and all wheels has actuated. Figure 1(a) shows the definition of the wheel number (We display as wheel i: $i = 1 \cdots 7$), the coordinates, the length of each links, and the rotate speed of each wheel, respectively. $R1$ and $R2$ indicate the length of each links and $\omega_1, \cdots, \omega_7$ are the rotation velocity of each wheel.

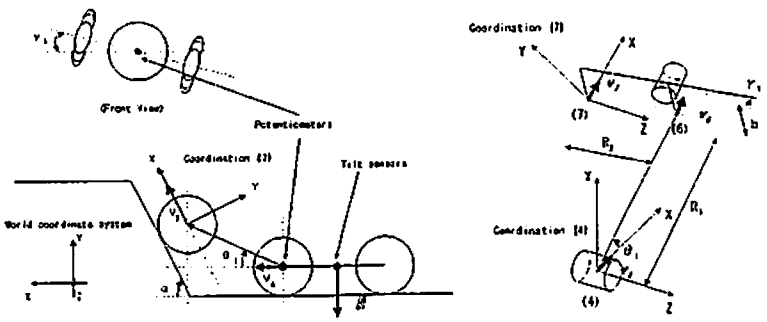

(a) Side view (b) 3D view

Fig. 3. Coordination and parameters of our prototype

When the vehicle runs at v_0 in x-direction on the coordination $\{4\}$, the velocity vector of wheel 7 on the coordination $\{4\}$ is derived as equation (7) by equation (1). The kinematic relationship among the wheels is shown in Figure 3(b).

$$
\begin{aligned}
{}^4\mathbf{v}_7 &= {}^4\mathbf{v}_6 + {}^4\sigma_6 \times {}^4\mathbf{P}_7^6 = ({}^4\mathbf{v}_4 + {}^4\sigma_4 \times {}^4\mathbf{P}_6^4) + {}^4\sigma_6 \times {}^4\mathbf{P}_7^6 \\
&= \begin{bmatrix} {}^4v_{7x} \\ {}^4v_{7y} \\ {}^4v_{7z} \end{bmatrix} = \begin{bmatrix} v_0 + \dot{\theta}_1 \{-R_1 \sin\theta_1 + R_2 \cos\theta_1 \sin\gamma_1 - b\cos\theta_1 (1 - \cos\gamma_1)\} \\ \dot{\theta}_1 \{R_1 \cos\theta_1 - R_2 \sin\theta_1 \sin\gamma_1 + b\sin\theta_1 (1 - \cos\gamma_1)\} - \dot{\gamma}_1 (R_2 \cos\gamma_1 - b\sin\gamma_1) \\ -\dot{\gamma}_1 (R_2 \cos\theta_1 \sin\gamma_1 - b\cos\theta_1 (1 - \cos\gamma_1)) \end{bmatrix}
\end{aligned} \tag{7}
$$

As the same, the velocity vectors of wheel 1, 3 and 5 are derived from equation (8), (9) and (10), respectively.

$$
{}^4\mathbf{v}_1 = \begin{bmatrix} {}^4v_{1x} \\ {}^4v_{1y} \\ {}^4v_{1z} \end{bmatrix} = \begin{bmatrix} v_0 - \dot{\theta}_2 \{R_1 \sin\theta_2 + R_2 \cos\theta_2 \sin\gamma_2 - b\cos\theta_2 (1 - \cos\gamma_2)\} \\ \dot{\theta}_2 \{R_1 \cos\theta_2 + R_2 \sin\theta_2 \sin\gamma_2 - b\sin\theta_2 (1 - \cos\gamma_2)\} + \dot{\gamma}_2 (R_2 \cos\gamma_2 - b\sin\gamma_2) \\ \dot{\gamma}_2 (R_2 \cos\theta_2 \sin\gamma_2 - b\cos\theta_2 (1 - \cos\gamma_2)) \end{bmatrix} \tag{8}
$$

$$
{}^4\mathbf{v}_3 = \begin{bmatrix} {}^4v_{3x} \\ {}^4v_{3y} \\ {}^4v_{3z} \end{bmatrix} = \begin{bmatrix} v_0 + \dot{\theta}_2 \{-R_1 \sin\theta_2 + R_2 \cos\theta_2 \sin\gamma_2 - b\cos\theta_2 (1 - \cos\gamma_2)\} \\ \dot{\theta}_2 \{R_1 \cos\theta_2 - R_2 \sin\theta_2 \sin\gamma_2 + b\sin\theta_2 (1 - \cos\gamma_2)\} - \dot{\gamma}_2 (R_2 \cos\gamma_2 - b\sin\gamma_2) \\ -\dot{\gamma}_2 (R_2 \cos\theta_2 \sin\gamma_2 - b\cos\theta_2 (1 - \cos\gamma_2)) \end{bmatrix} \tag{9}
$$

$$
{}^4\mathbf{v}_5 = \begin{bmatrix} {}^4v_{5x} \\ {}^4v_{5y} \\ {}^4v_{5z} \end{bmatrix} = \begin{bmatrix} v_0 - \dot{\theta}_1 \{R_1 \sin\theta_1 + R_2 \cos\theta_1 \sin\gamma_1 - b\cos\theta_1 (1 - \cos\gamma_1)\} \\ \dot{\theta}_1 \{R_1 \cos\theta_1 + R_2 \sin\theta_1 \sin\gamma_1 - b\sin\theta_1 (1 - \cos\gamma_1)\} + \dot{\gamma}_1 (R_2 \cos\gamma_1 - b\sin\gamma_1) \\ \dot{\gamma}_1 (R_2 \cos\theta_1 \sin\gamma_1 - b\cos\theta_1 (1 - \cos\gamma_1)) \end{bmatrix} \tag{10}
$$

On the other hand, the rotation vector of each wheel is derived using the roll and pitch angle as shown in equation (11) and (12). In equation (11), The rotation vectors of wheel 5 and 7 are same because these wheels are connected by same linkages. As the same, the rotation vectors of the wheel 1 and 3 are same in equation (12).

$$
{}^4\sigma_5 = {}^4\sigma_7 = \begin{bmatrix} {}^4\sigma_{7x} & {}^4\sigma_{7y} & {}^4\sigma_{7z} \end{bmatrix}^T = \begin{bmatrix} \dot{\gamma}_1 & 0 & \dot{\theta}_1 \end{bmatrix}^T \tag{11}
$$

$$
{}^4\sigma_1 = {}^4\sigma_3 = \begin{bmatrix} {}^4\sigma_{3x} & {}^4\sigma_{3y} & {}^4\sigma_{3z} \end{bmatrix}^T = \begin{bmatrix} \dot{\gamma}_2 & 0 & \dot{\theta}_2 \end{bmatrix}^T \tag{12}
$$

2.3 Derivation of Wheel Control Reference

In previous section, we derive the velocity vectors and rotation vector of each wheel when the vehicle runs at v_0 on the coordination $\{4\}$. However, these vectors are only calculated by kinematical relationship of wheels and the velocity vector of wheel, which passes over the step, tends to become extraordinary because of change of body shape. If we derive the wheel control reference by these extraordinary vectors using equation (4) simply, wheel control references become also extraordinary and cause wheel slippage and rotation error. In order to derive suitable wheel control references from results of previous section, we consider the following points.

- When the vehicle passes over the step at V_0 in advanced direction on the vehicle coordination as shown in Figure 1 (a), we set V_0 as the velocity in x-direction on the coordination $\{4\}$.

- All wheel velocity based on V_0 referring to body configuration must be smaller than V_0.

Our proposed scheme is shown in Figure 4. When the vehicle passes over the step at V_0 on the vehicle coordination as shown in Figure 1 (a), we set the velocity in x-direction on the coordination $\{4\}$ as equation (13) temporary and we derive the velocity vectors of all wheels from equation (7)-(10).

$$^4v_{4x} = V_0 \tag{13}$$

The coefficient c_i of wheel i is determined by equation (14).

$$c_i = \begin{cases} \frac{|V_0|}{|^4\mathbf{v}_i|} & if\ |^4\mathbf{v}_i| > |V_0| \\ 1 & if\ |^4\mathbf{v}_i| \leq |V_0| \end{cases} \tag{14}$$

where $^4\mathbf{v}_i$ indicates the calculated velocity vector of wheel i. i $(= 1, \cdots, 7)$ means sub-number for identification of the wheel.

The velocity vector on the coordination $\{4\}$ is determined by equation (15). Using equation (15), all wheel velocity vectors are calculated within the range of V_0.

$$\mathbf{v}_i^{out} = c \cdot {}^4\mathbf{v}_i \tag{15}$$

where $c = \min\{c_1, \cdots, c_7\}$.

Now, we derive the wheel control references from wheel velocity vector and rotation vector derived in previous section. When we set v_0 as the velocity vector $\mathbf{v}_4^{out}$ of x-direction, the velocity vector of wheel i on the coordination $\{i\}$ is shown in equation (16). As shown in equation (5), we assume that the obstacle is the α-degree slope about each wheel as shown in Figure 3(a).

$$^i\mathbf{v}_i = {}_4^i\mathbf{R} \cdot {}^4\mathbf{v}_i = \begin{bmatrix} \cos\alpha & -\sin\alpha & 0 \\ \sin\alpha & \cos\alpha & 0 \\ 0 & 0 & 1 \end{bmatrix} \cdot \begin{bmatrix} ^4v_{ix} \\ ^4v_{iy} \\ ^4v_{iz} \end{bmatrix} = \begin{bmatrix} \cos\alpha \cdot {}^4v_{ix} - \sin\alpha \cdot {}^4v_{iy} \\ \sin\alpha \cdot {}^4v_{ix} + \cos\alpha \cdot {}^4v_{iy} \\ ^4v_{iz} \end{bmatrix} \tag{16}$$

From equation (4) and (13), the control reference of wheel i is expressed in equation (17).

$$\omega_i = \frac{\cos\alpha \cdot {}^4v_{ix} - \sin\alpha \cdot {}^4v_{iy}}{r} + {}^4\sigma_{iz} \tag{17}$$

The α-degree is defined in equation (18), because the x-axis is defined in the drive direction of the wheel and the velocity vector is parallel to the drive direction as equation (6).

$$\sin\alpha \cdot {}^4v_{ix} + \cos\alpha \cdot {}^4v_{iy} = 0 \tag{18}$$

Our vehicle controls each wheel based on this control reference using PID based control system. [8]

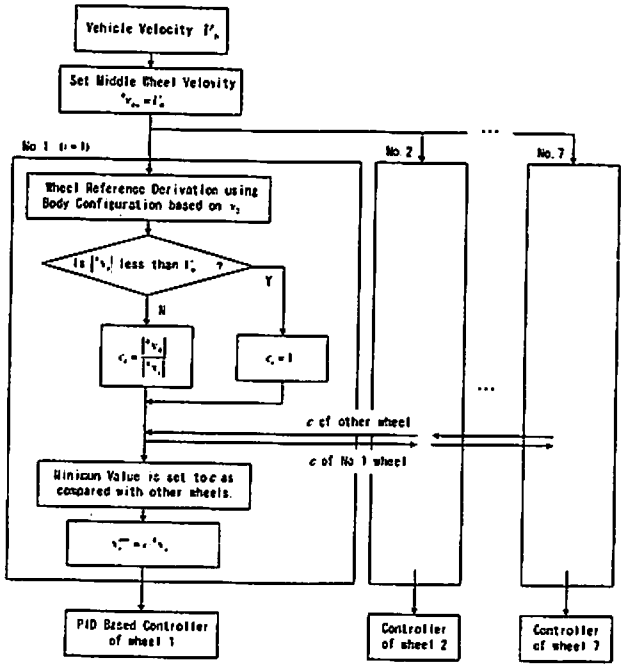

Fig. 4. Flow chart of the wheel control reference derivation

3 Experiments

3.1 Computer Simulation

We verify the effectiveness of our proposed control reference by computer simulations. We adapt our proposed control reference to test vehicle model and compare the result of proposed reference with the result of fixed reference which does not consider the body configuration. As initial conditions, simulation parameters of test vehicle model are chosen from our prototype model. The parameters are shown in Table 1.

Table 1. Parameters of prototype

Number of Linkages	2
Length of Linkage	Front Part 195[mm], Rear Part 400[mm]
Body Weight	Front Part 7.8[kg], Rear Part 13.8[kg]
Wheel Diameter	132[mm]
Distance between Wheels	Front-Middle 255[mm], Middle-Rear 215[mm]
Friction Coefficient	Static 0.3, Dynamic 0.25
Running Speed (V_0)	0.25[m/sec]

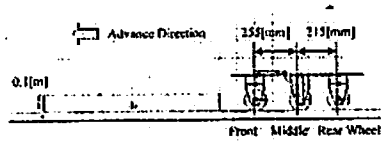

Fig. 5. Simulation setup

In this simulation, the vehicle passes over the step at advance direction as shown in Figure 5. The vertical gap of step is 0.1[m].

We use the Working Model 2D as a physical simulator and MATLAB as a controller. Working Model calculates the vehicle conditions dynamically using Kutta-Merson integrator and outputs the sensing data for MATLAB such as rotational velocities of each wheel and angle of free joint. MATLAB calculates the output value of each actuator using these values with our developed PID based controller [12] and returns the output value for Working Model. Both applications are linked by Dynamic Data Exchange function on MS Windows.

3.2 Simulation Results

As the result of the simulation, when the prototype vehicle passes over the 0.1[m] height step, control references of each wheel are derived as shown in Figure 6. These references are within the range of V_0 and we verify these control references are suitable.

Figure 7 shows the slippage ratio and Figure 8 shows rotation error ratio of the wheels during step climbing. The slippage ratio of the wheel decreases 54[%] and the rotation error ratio of the wheel decreases 55[%] by our proposed control method as shown in Table 2. The slip ratio and the rotation error ratio of wheel are calculated by equation (19) and (20), respectively.

$$\hat{s} = \frac{r\omega - v_\omega}{r\omega} \tag{19}$$

$$\hat{d} = \frac{\omega_{ref} - \omega}{\omega} \tag{20}$$

where ω is the rotation velocity of the wheel and ω_{ref} is the reference value of wheel rotation velocity. r and v_ω indicate the radius of the wheel and the vehicle speed, respectively.

From these results, our proposed method reduces the slippage and the rotation error of the wheels. Therefore, our proposed control method is effective for increasing the mobile performance of the vehicle during step-climbing.

3.3 Experiments

Here, we verify the mobile performance of proposed wheel control method by the experiments using our prototype. In this experiment, the vehicle passes

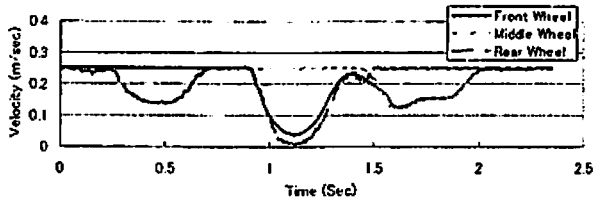

Fig. 6. Wheel control reference during step-climbing

Table 2. Slippage and rotation error ratio of wheel [%]

	Method	Front Wheel	Middle Wheel	Rear Wheel	Average
Slippage Ratio	Standard	31.3	30.3	29.6	30.3
	Proposed	13.1	14.3	14.2	13.9
Rotation Error Ratio	Standard	16.5	16.3	16.6	16.5
	Proposed	7.4	7.2	7.9	7.5

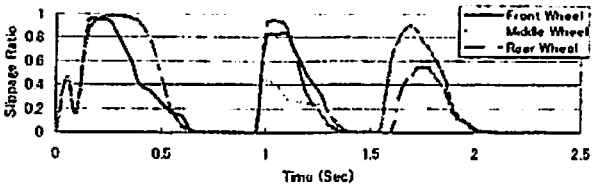

(a) With standard control method

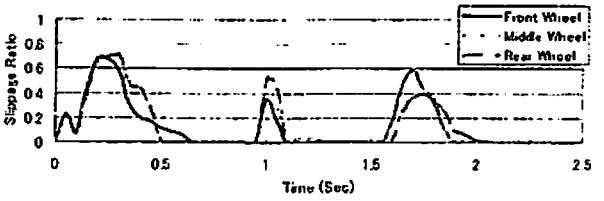

(b) With proposed control method

Fig. 7. Wheel slippage ratio

over the step in advance direction and we verify the height of the step which the vehicle can climb up. Experimental conditions are same as the prototype vehicle parameters shown in Table 1. We compare the results by our proposed method with the result utilizing standard PID controller, which doesn't consider the body configuration.

As the result of the experiment, the vehicle can pass over the 0.152[m] height step with our proposed wheel control method as shown in Figure 9. With standard method, the vehicle can pass over the only 0.072[m] height

and its step-overcoming performance is improved. As the results, our vehicle realizes 152[mm] height step-climbing performance with wheel of 132[mm] diameter. Its performance is useful for omni-directional wheeled vehicle. Our proposed wheel control method can utilize for the vehicle which has passive suspension mechanism.

References

1. G. Campion, G. Bastin and B.D. Andrea-Novel. Structual Properties and Classification of Kinematic and Dynamic Models of Wheeled Mobile Robots. In: IEEE Trans. on Robotics and Automation, Vol.12, No.1, pp.47–62, 1996.
2. M. Ichikawa. Wheel arrangements for Wheeled Vehicle. Journal of the Robotics Society of Japan, Vol.13, No.1, pp.107–112, 1995.
3. G. Endo and S. Hirose. Study on Roller-Walker: System Integration and Basic Experiments, In: Proc. of the 1999 IEEE Int. Conf. on Robotics & Automation, pp.2032-2037, 1999.
4. T. McGeer. Passive dynamic walking, The Int. Journal of Robotics Research, vol.9, No.2, pp62-82, 1990.
5. M. Wada and H. Asada. Design and Control of a Variable Footpoint Mechanism for Holonomic Omnidirectional Vehicles and its Application to Wheelchairs. In: IEEE Trans. on Robotics and Automation, Vol.15, No.6, pp.978-989, 1999.
6. S. Hirose and S. Amano. The VUTON: High Payload, High Efficiency Holonomic Omni-Directional Vehicle. In: Proc. of the 6th Symp. on Robotics Research, pp.253-260, 1993.
7. D. Chugo, *et al.* Development of omni-directional vehicle with step-climbing ability. In: Proc. of the 2003 IEEE Int. Conf. on Robotics & Automation, pp.3849–3854, 2003.
8. H. Asama, *et al.* Development of an Omni-Directional Mobile Robot with 3 DOF Decoupling Drive Mechanism. In: Proc. of the 1995 IEEE Int. Conf. on Robotics and Automation, pp.1925–1930, 1995.
9. Stone, H. W., Mars Pathfinder Microrover: A Low-Cost, Low-Power Spacecraft, In: Proc. of the 1996 AIAA Forum on Advanced Developments in Space Robotics, 1996.
10. Y.Kuroda, *et al.* Low Power Mobility System for Micro Planetary Rover Micro5. In: Proc. of the 5th Int. Symp. on Artificial Intelligence, Robotics and Automation in Space (i-SAIRAS99), pp.77–82, 1999.
11. Brian Carisle, An Omni-Directional Mobile Robot. Developments in Robotics 1983, IFS Publications Ltd., pp.79–87, 1983.
12. D. Chugo, *et al.* Development of Control System for Omni directional Vehicle with Step-Climbing Ability. In: Proc. of the 4th Int. Conf. on Field and Service Robotics, pp.121–126, 2003.
13. P. Lamon, *et al.* Wheel torque control for a rough terrain rover. In: Proc. of the Int. Conf. on Robotics and Automation, pp.4682–4687, 2004.
14. D. Chugo, *et al.* Vehicle Control Based on Body Configuration. In: Proc. of the IEEE/RSJ Int. Conf. on Intelligent Robots and Systems, pp.1493–1498, 2004.
15. K.Yoshida and H.Hamano. Motion Dynamic of a Rover With Slip-Based Traction Model. In: Proc. of the 2002 IEEE Int. Conf. on Robotics & Automation, pp.3155–3160, 2001.